REPORT DOCUMENTATION PAGE

Form Approved OMB NO. 0704-0188

1. REPORT DATE (DD-MM-YYYY)	2. REPORT TYPE	3. DATES COVERED (From - To)
17-02-2011	Final Report	1-Jul-2007 - 30-Dec-2010

4. TITLE AND SUBTITLE
Final Report for W911NF0710458

5a. CONTRACT NUMBER
W911NF-07-1-0458

5b. GRANT NUMBER

5c. PROGRAM ELEMENT NUMBER
611102

6. AUTHORS
Manish Chhowalla

5d. PROJECT NUMBER

5e. TASK NUMBER

5f. WORK UNIT NUMBER

7. PERFORMING ORGANIZATION NAMES AND ADDRESSES
Rutgers, The State University of New Jersey - Pis
Office Of Research & Sponsored Programs
58 Bevier Road
Piscataway, NJ 08854 -8010

8. PERFORMING ORGANIZATION REPORT NUMBER

9. SPONSORING/MONITORING AGENCY NAME(S) AND ADDRESS(ES)
U.S. Army Research Office
P.O. Box 12211
Research Triangle Park, NC 27709-2211

10. SPONSOR/MONITOR'S ACRONYM(S)
ARO

11. SPONSOR/MONITOR'S REPORT NUMBER(S)
49635-MS.1

12. DISTRIBUTION AVAILIBILITY STATEMENT
Approved for Public Release; Distribution Unlimited

13. SUPPLEMENTARY NOTES
The views, opinions and/or findings contained in this report are those of the author(s) and should not contrued as an official Department of the Army position, policy or decision, unless so designated by other documentation.

14. ABSTRACT
This report contains the following results:

1.Demonstration of novel synthesis method that allows deposition of boron carbide with lower graphitic and amorphous carbon inclusions.
2.Synthesis of silicon doped boron carbide.

15. SUBJECT TERMS
boron carbide, ballistic impact, nanostructures

16. SECURITY CLASSIFICATION OF:			17. LIMITATION OF ABSTRACT	15. NUMBER OF PAGES	19a. NAME OF RESPONSIBLE PERSON
a. REPORT	b. ABSTRACT	c. THIS PAGE			Manish Chhowalla
UU	UU	UU	UU		19b. TELEPHONE NUMBER: 732-445-5619

Report Title

Final Report for W911NF0710458

ABSTRACT

This report contains the following results:

1.Demonstration of novel synthesis method that allows deposition of boron carbide with lower graphitic and amorphous carbon inclusions.
2.Synthesis of silicon doped boron carbide.
3.Spark plasma sintering of nearly fully dense silicon doped boron carbide without any sintering aids
4.Demonstration of minimal electric shock induced amorphization in the silicon doped SPS material
5.Demonstration of much lower amorphization under static indentation loading

List of papers submitted or published that acknowledge ARO support during this reporting period. List the papers, including journal references, in the following categories:

(a) Papers published in peer-reviewed journals (N/A for none)

Number of Papers published in peer-reviewed journals: 0.00

(b) Papers published in non-peer-reviewed journals or in conference proceedings (N/A for none)

Number of Papers published in non peer-reviewed journals: 0.00

(c) Presentations

Number of Presentations: 0.00

Non Peer-Reviewed Conference Proceeding publications (other than abstracts):

Number of Non Peer-Reviewed Conference Proceeding publications (other than abstracts): 0

Peer-Reviewed Conference Proceeding publications (other than abstracts):

Number of Peer-Reviewed Conference Proceeding publications (other than abstracts): 0

(d) Manuscripts

Number of Manuscripts: 0.00

Patents Submitted

Patents Awarded

Awards

Graduate Students

NAME	PERCENT_SUPPORTED
Sara Reynaud	1.00
FTE Equivalent:	**1.00**
Total Number:	**1**

Names of Post Doctorates

NAME	PERCENT_SUPPORTED
Hisato Yamaguchi	0.50
FTE Equivalent:	**0.50**
Total Number:	**1**

Names of Faculty Supported

NAME	PERCENT_SUPPORTED	National Academy Member
Manish Chhowalla	0.00	No
FTE Equivalent:	**0.00**	
Total Number:	**1**	

Names of Under Graduate students supported

NAME	PERCENT_SUPPORTED
FTE Equivalent:	
Total Number:	

Student Metrics

This section only applies to graduating undergraduates supported by this agreement in this reporting period

The number of undergraduates funded by this agreement who graduated during this period:	0.00
The number of undergraduates funded by this agreement who graduated during this period with a degree in science, mathematics, engineering, or technology fields:	0.00
The number of undergraduates funded by your agreement who graduated during this period and will continue to pursue a graduate or Ph.D. degree in science, mathematics, engineering, or technology fields:	0.00
Number of graduating undergraduates who achieved a 3.5 GPA to 4.0 (4.0 max scale):	0.00
Number of graduating undergraduates funded by a DoD funded Center of Excellence grant for Education, Research and Engineering:	0.00
The number of undergraduates funded by your agreement who graduated during this period and intend to work for the Department of Defense	0.00
The number of undergraduates funded by your agreement who graduated during this period and will receive scholarships or fellowships for further studies in science, mathematics, engineering or technology fields:	0.00

Names of Personnel receiving masters degrees

NAME
Total Number:

Names of personnel receiving PHDs

NAME	
Sara Reynaud	
Total Number:	**1**

Names of other research staff

NAME	PERCENT_SUPPORTED
FTE Equivalent:	
Total Number:	

Sub Contractors (DD882)

Inventions (DD882)

Scientific Progress

During this no cost extension, we finalized the results of the project and confirmed the contents of the final report. We are also in the process of finalizing (within a week or two) a Review MS on boron carbide that will be submitted to the Journal of American Ceramic Society. The Review MS is the result of the detailed literature survey performed by Sara Reynaud for her thesis.

Technology Transfer

Final Report (Jan 2011)

ARO Reference number: W911NF0710458

Point of contact: Professor Manish Chhowalla

Contact address: Rutgers University, Department of Materials Science and Engineering, Piscataway, NJ 08854, USA, 732 445 5619, Email: manish1@rci.rutgers.edu

Primary Objectives Achieved:

1. Demonstration of novel synthesis method that allows deposition of boron carbide with lower graphitic and amorphous carbon inclusions.
2. Synthesis of silicon doped boron carbide.
3. Spark plasma sintering of nearly fully dense silicon doped boron carbide without any sintering aids
4. Demonstration of minimal electric shock induced amorphization in the silicon doped SPS material
5. Demonstration of much lower amorphization under static indentation loading

Background

In our previous work, we provided an explanation for the absence of a plastic phase in boron carbide and its dynamic failure at threat velocities just above the Hugoniot elastic limit (H_{EL}) [1]. Using self-consistent field density functional simulations we were able to account for many experimental observations by demonstrating that several boron carbide polytypes [$(B_{11}C)C_2B$, $(B_{12})C_3$, etc.] can coexist without significant lattice distortions (See Figure 1). Our analysis indicated that above a threshold pressure all the candidate polytypes are less stable than a phase involving segregated boron (B_{12}) and amorphous carbon (a-C) but the energetic barrier between boron carbide and B_{12} + 3C, is by far lower for the B_{12}(CCC) polytype, requiring the lowest atomic displacement for $B_4C \rightarrow 3B+a\text{-}C$ transformation, occurring at pressures of 6 GPa ≈ $P(H_{EL})$. For such a configuration, segregation of free carbon occurs in layers orthogonal to the (113) lattice directions, in excellent agreement with recent transmission electron microscopy (TEM) analysis [2]. In other words, the B_{12}(CCC) polytype acts as the weak link leading to the premature failure of boron carbide. Therefore, to improve the ballistic performance of boron carbide, it is necessary to eliminate the B_{12}(CCC) polytype. Thus, the root mechanism leading to premature failure of boron carbide was identified, opening up the possibility of tailoring its properties through careful reduction of disorder during synthesis. However, thermal disorder is unavoidable during synthesis and hot pressing of boron carbide.

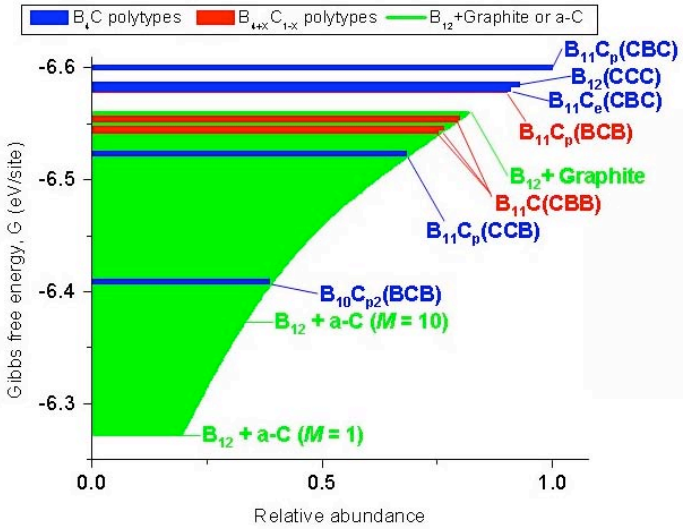

Figure 1: Gibbs free energy vs. relative abundance of the most significant polytypes. Since the materials are synthesized at temperatures T_s > 2000 K, the disorder potential can be estimated to be $\Delta V \approx k_B T_s$ > 0.2 eV.

To provide a solution for improved impact performance of boron carbide, we have studied the effects of Si doping. The Gibbs free energy of the $B_{11}C_p$(CBC) and B_{12}(CCC) polytypes as a function of substitutional Si doping is shown in Figure 2. It can be observed that the difference in Gibbs free energy between the stable polytype, $B_{11}C_{(1-y,p)}Si_{(y,p)}$(CBC) and the most energetically favored minority polytype $B_{12}(CSi_yC_{(1-y)}C)$, strongly increases by a factor of 15, from ΔG = 0.015 eV at 0 at.% Si (see also Fig. 1) to ΔG = 0.23 eV at 6.7 at.% Si. Hence, in the latter case, the concentration of the minority polytype decreases by $\exp(-15) \approx 3 \cdot 10^{-7}$ times in the presence of Si. Thus, the B_{12}(CCC) polytype leading to the premature failure in boron carbide can be practically completely eliminated via incorporation of Si. In contrast, the force on the atoms and their derivatives only experience negligible variations, indicating that the elastic constants do

not experience large modifications at sufficiently low Si doping. Therefore, experimental realization of Si-containing boron carbide could lead to the development of a material with HEL exceeding 40 GPa. This would make it an excellent material for protection against high-energy impacts, for instance as a blast shield against terrorist devices or as ballistic armor in military applications or for increased safety when vehicles collide.

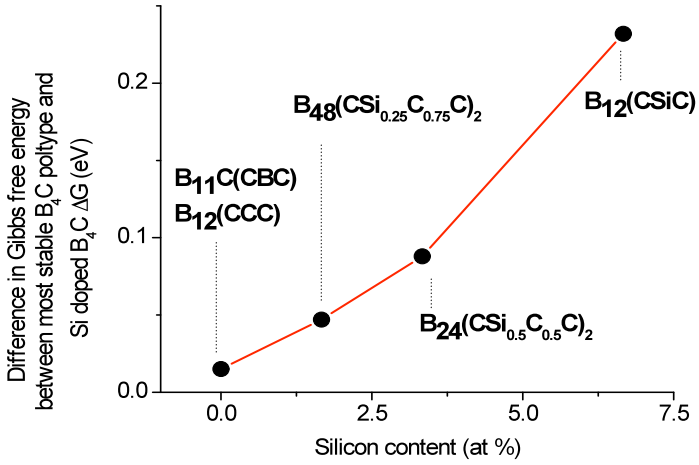

Figure 2: Gibbs free energy of the $B_{11}C_p(CBC)$ and $B_{12}(CCC)$ polytypes as a function of silicon atom concentration. It can be observed that the difference in Gibbs free energy between the stable polytype, B_{11} $C_{(1-y,p)}Si_{(y,p)}(CBC)$ and the most energetically favored minority polytype, $B_{12}(CSi_yC_{1-y}C)$ increase with the silicon content. Hence silicon-containing boron carbide is less affected by disorder than the undoped one.

In the second stage of our understanding, we determined that Si addition to boron carbide could prevent the formation of the $B_{12}(CCC)$ polytype, thus inhibiting the segregation of amorphous carbon and graphite and stabilizing the material against high stresses and shocks.

Synthesis of materials

Si-doping of boron carbide, although claimed to be attained in the past, is generally assessed to be difficult due to the strong stability of silicon-carbon and silicon-boron compounds (i.e. SiC and boro-silicates) which tend to segregate. Therefore, although it is easy to attain $B_4C_{1-x}Si_x$ stoichiometries, it is not straightforward that they correspond to a homogeneous compound with the icosahedral structure of B_4C in which Si acts as a substitutional dopant.

To achieve this goal we explored the synthesis of boron carbide via the solid-liquid-solid (SLS) method [3], exploiting the relative low temperature of the Ni-Co-B_4Si quaternary eutectic (i.e. about 950^{o}C, Fig. 3). The process is widely used to prepare a wide range of nanostructured materials, such as silicon and germanium nanowires. It consists of the formation of a sutectic droplet, which acts to catalyze the nanowire growth. That is, at the appropriate thermodynamic conditions, the reacts migrate to the liquid catalyst until it is supersaturated. Additional reactants above the supersaturated phase are precipitated out in the form of nanowires.

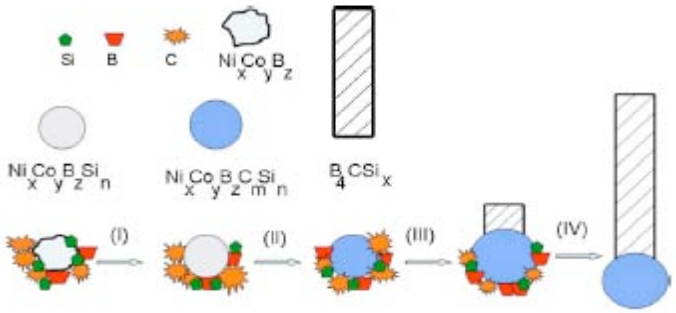

Figure 3: Schematic of the solid-liquid-solid (SLS) mechanism used for the growth of Si-doped B_4C nanowires.

The furnace for growing the Si doped B_4C nanoparticles has been setup as follows: a crucible containing the finely ground reagents is placed at the center of a furnace. Subsequently, Ar is admitted to the furnace at a controlled flow rate and the furnace is heated up to the synthesis temperature.

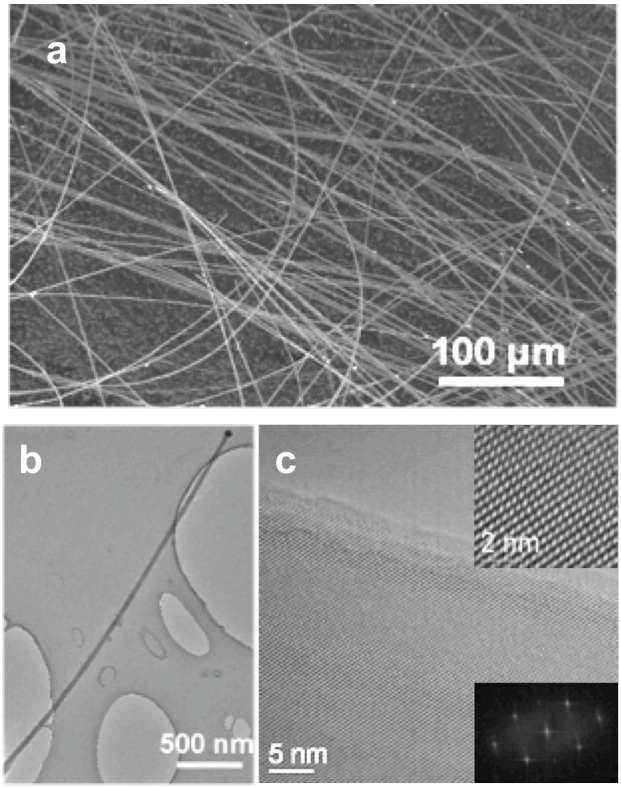

Figure 4: SEM and TEM images of silicon doped boron carbide nanowires.

The scanning electron microscopy (SEM) image in Figure 4a show typical nanowires obtained using the SLS technique. In the solid-liquid-solid (SLS) method of B_4C NWs, the overall yield of the NWs is tens of milligrams for 1 gram of starting precursors. We found two regimes of growth. The first was what we refer to as typical NWs with diameters ranging from 10 nm – 100 nm and lengths ranging from 1 – 10 µm. To make sizable quantities of nanowires for project such as this one, we typically utilize several boats within the tube furnace and run multiple growth cycles. The transmission electron microscopy images in Figures 4b and 4c show that the NWs are of very high crystalline quality, with the structure obtained from the calculated diffraction pattern in agreement with that of $B_{4.3}C$. The compositional profile of the nanowires was obtained using electron dispersive spectroscopy (EDX) in a scanning TEM with a focused probe of 1 nm (see colorful images below in Figure 5). It can be seen that the tip of the NW contains the eutectic composition of the catalyst but the NW is mostly boron carbon doped with silicon. The composition of silicon was estimated to be ~ 2.3 at. %, which is consistent with

simulations. The above suggests that it is possible to dope boron carbide with silicon without disturbing the boron carbide structure. Although we have performed detailed analysis of the structure of the silicon doped nanowires and confirmed it to be that of boron carbide, the possibility of the formation of SiC cannot be completely ruled out. The Raman spectrum of the silicon-doped boron carbide is substantially different from that of commercial boron carbide powders, which contain a sizable amount of amorphous carbon. This also suggests that the nanowires are of very crystallinity. More details about the Raman spectra of boron carbide are given below.

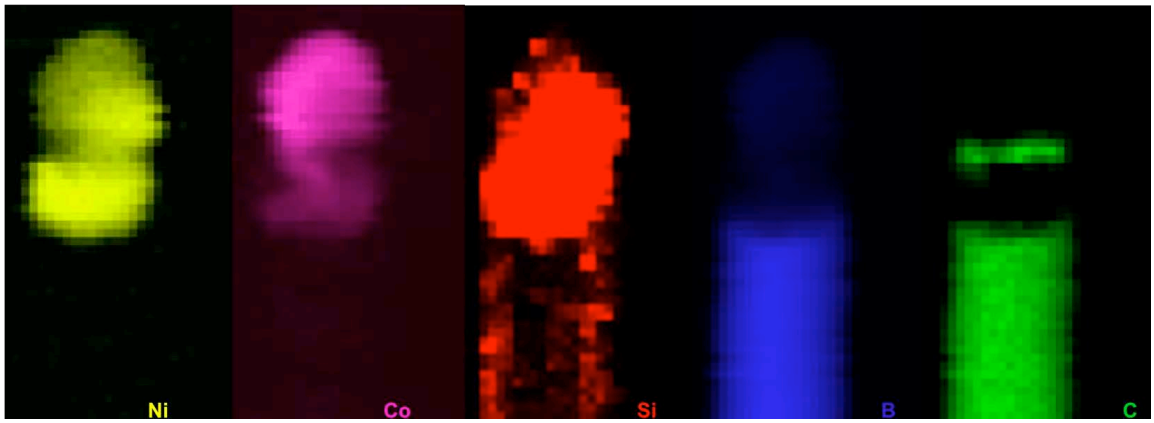

Figure 5: Compositional profile of boron carbide nanowires containing silicon.

Consolidation by spark plasma sintering

Based on our simulations, the silicon doped boron carbide nanowires are metastable (Figure 2). Therefore any additional processing for consolidation will require a technique that is able to preserve the meta-stability of the silicon doped nanowires. Traditional hot pressing is unlikely to achieve this as the powder is typically held at high temperatures for an hour or more, sufficient time for any metastable phases to relax to their most energetically favorable conditions. Approximately 10grams of the powder was produced and ball milled to homogenize the size distribution. The powder was then placed into spark plasma sintering (SPS) system for consolidation. Two samples were densified at 2100^{o}C (SPS No.1477) and 2175^{o}C (SPS No.1479) under 50MPa for 20 min. The SPS parameters for one consolidation heating and cooling cycle are shown in Figure 6. The vacuum level is not shown in Figure 6 but a loss of vacuum was observed for all cycles. The source of outgassing at high temperatures will require further investigation. It should be noted that no sintering aids were added to the powder. The samples were in the form of disks (diameter = 2cm and thickness ~ 4mm, see photograph below). The densities of the samples measured by the Archimedes method (2.5 g-cm^{-3} ± 0.1) were found to be very similar and also close to the theoretical value (2.52 g-cm^{-3}).

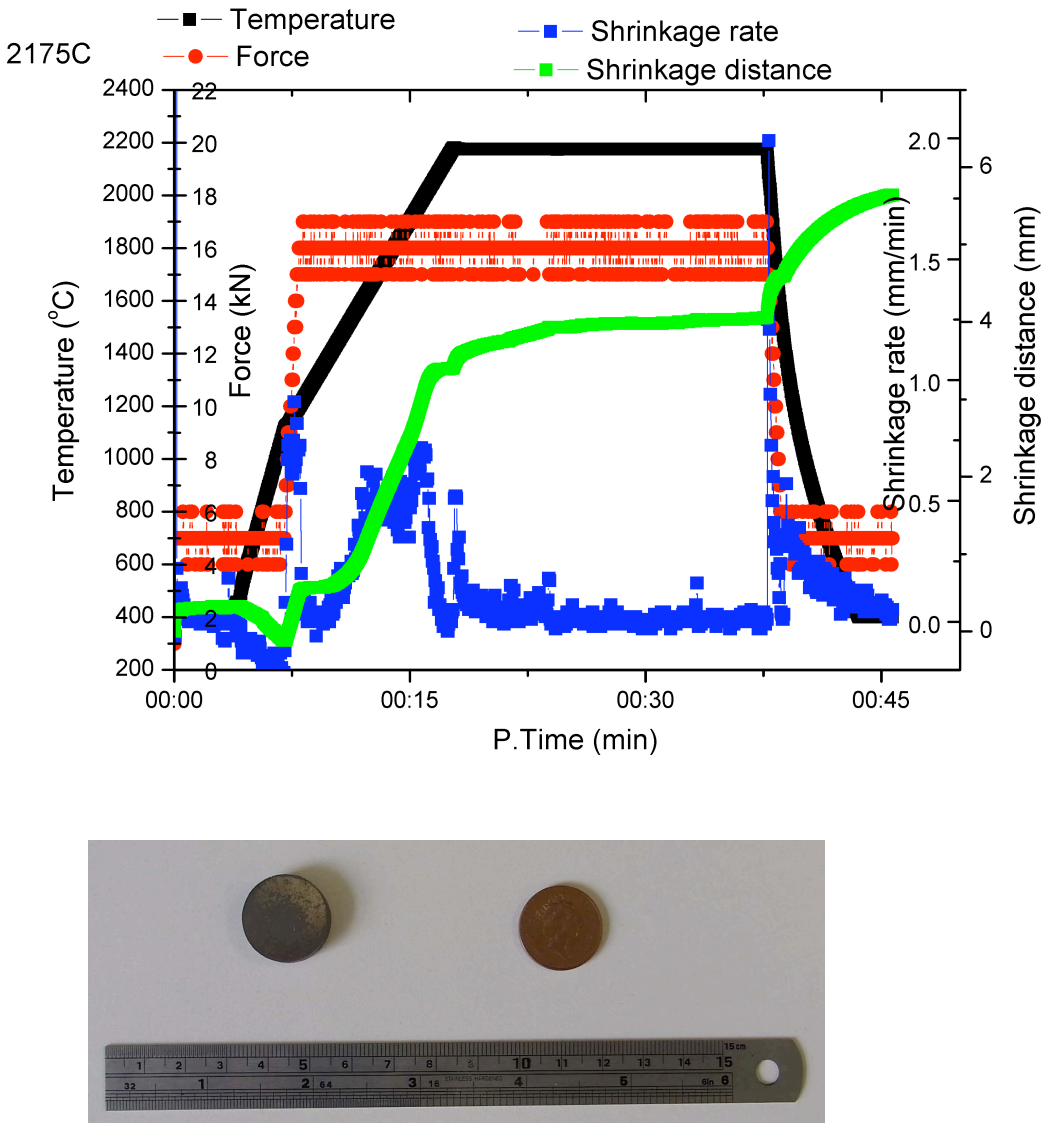

Figure 6: Spark plasma sintering cycle of silicon doped nanowires. Below is an image of the consolidated component.

Microstructure of SPS consolidated Si-doped B4C

A fracture surface showing the microstructure of the SPS consolidated Si-doped B_4C is shown in Figure 7. The scale bar in the figure indicates 500nm, suggesting that the NWs fuse together to form sub-micron or nanoscale grains, retaining the original properties of the starting powder. The microstructures of the two consolidated samples were found to be similar and no obvious differences in the SEM could be observed. However, a more detailed study for closer examination of the microstructure is warranted.

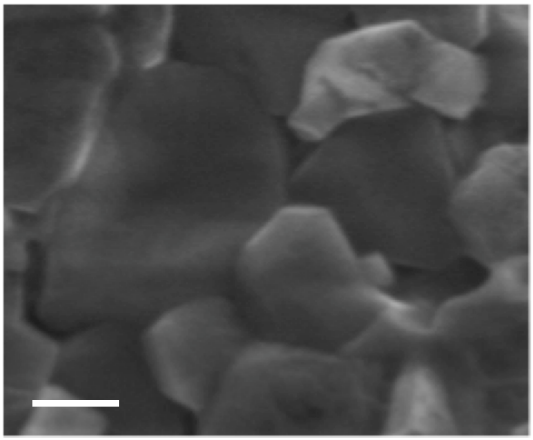

Figure 7: Microstructure of SPS consolidated Si-doped B4C.

Raman of B_4C

Raman spectroscopy has been widely used to characterize B_4C, which owing to its complex crystallographic structure gives rise to a number of Raman-active vibrations at and below 1150 cm^{-1}. Thus, Raman contributions of B_4C are easily distinguishable from the modes of the aromatic sp^2 clusters found at higher frequencies. Although some controversy remains on the origin of some B_4C peaks, all the studies performed to date agree that the strong peak at ~1100 cm^{-1} can be assigned to the icosahedron breathing mode (IBM) (Figure 8). The other B_4C modes are found at 275-325 cm^{-1} (origin of which will be discussed elsewhere), at 480 cm^{-1} (attributed to C-B-C chain stretching mode), and at 525 cm^{-1} (the icosahedral libration mode). The latter two peaks are strongly dependent on the orientation of the B_4C microcrystals with respect to the Raman laser beam, but they generally scale in intensity with the IBM mode. A similar scaling behavior is also observed for the other B_4C modes at 650-1000 cm^{-1}.

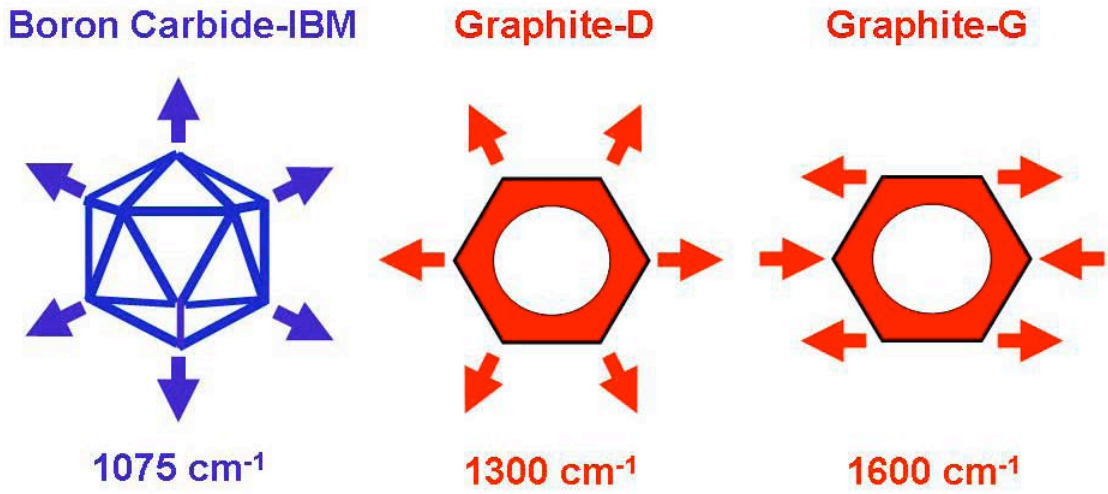

Figure 8: Schematic of stretchings that give rise to the various Raman peaks observed in the spectra of boron carbide.

In addition to information about the boron carbide phase, substantial insight into

the presence of free carbon in B_4C can also be obtained by careful Raman analysis. The first-order Raman spectrum of graphite single crystals shows only one peak at 1589 cm^{-1} (G-peak), which is the fingerprint of stretching vibrations of double, C=C, bonds. In the presence of graphitic domains of finite size, amorphization of the graphene layer, or defects, a second peak appears at 1300-1360 cm^{-1} (D-peak). This peak can be assigned to breathing vibrations of aromatic 6-fold rings in finite graphitic domains. In particular, it has been shown that at visible or near infrared excitation wavelength, λ, the diameter, L, of the sp^2 domain is related to the D/G intensity ratio.

Using the above, we have analyzed the amount of free carbon in commercial powders and hot pressed samples. As shown in Figure 9, the Raman spectra of the hot pressed sample do not substantially differ from those of the powder. Specifically, Figure 8a shows that there is little or no difference between the boron-carbide related peaks of the powder and of the solid sample both in relative intensity and or frequency positions. Similarly, the peaks arising from the sp^2 carbon phase of the hot pressed sample approximately undergo the same statistical fluctuations observed for the powder. Thus, the average carbon portion of the Raman spectra is also comparable for the powder and the densified sample, as shown in Figure 9b where two low-resolution Raman spectra from powder and hot-pressed samples are compared. This indicates that neither hot pressing nor sample cutting introduced significant amount of carbon inclusions in the densified sample. In addition, since our surface has been cut through the center of the tile, we may rule out that the observed sp^2 carbon clusters arise from surface carbon contamination.

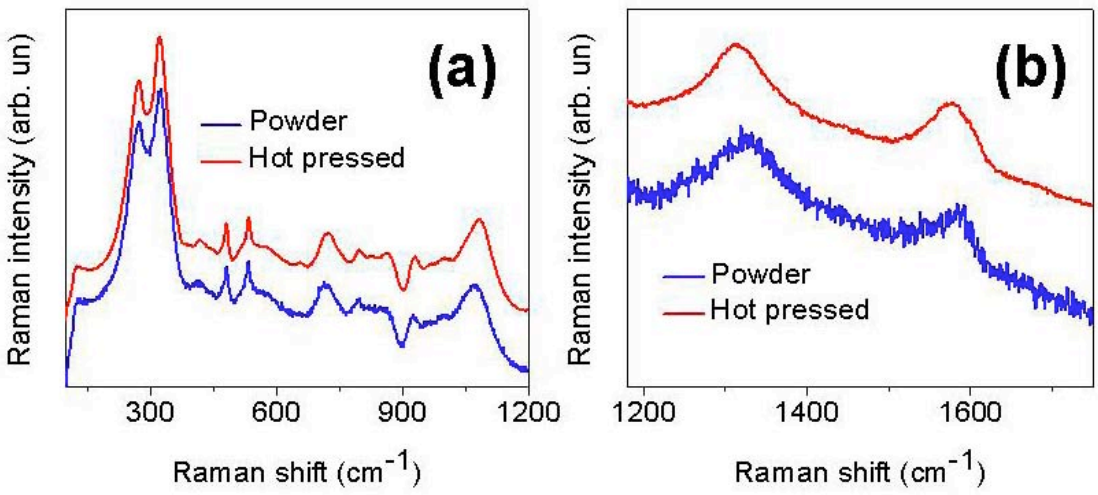

Figure 9: Raman spectra of commercially available B_4C powder and hot pressed samples. The left hand side is the B_4C portion of the spectra while the right panel shows the Raman D and G peaks attributed to the presence of amorphous carbon.

Failure and Amorphization in SPS consolidated Si-doped B4C

Postmortem analysis of impacted boron carbide samples generally reveals the presence of amorphous carbon phase. TEM analysis by Chen et al. revealed that the failure occurs as amorphous bands along the 113 directions [2]. The bands consist of B_{12} icosadehra collapsed within amorphous carbon. Thus a quick way to obtain insight into

the failure mode of B_4C is to monitor the degree of amorphous carbon in as consolidated B_4C. Several techniques using static and dynamic indentations have been employed to predict the quality of boron carbide. Domnich et al. [4] utilized *ex-situ* Raman measurements to characterize local graphitization induced by nanoindentation. They showed that graphitization does not occur until a pressure of approximately 40GPa, twice the value of B_4C failure under impact. Therefore, real time characterization of the graphitization process could provide valuable insight into why B_4C fails prematurely in dynamic tests. In this work, we show that graphitization in B_4C can occur by the application of relatively low electric fields. By applying pulses of increasing voltage and simultaneously monitoring phase changes with Raman spectroscopy (Figure 10a), it is possible to observe not only the onset but also the degree of graphitization in real time. Furthermore, through electrical measurements as a function of temperature in conjunction with Raman spectroscopy, we are able to determine that above a critical electrical field, the graphitization leads to the collapse of the B_4C structure.

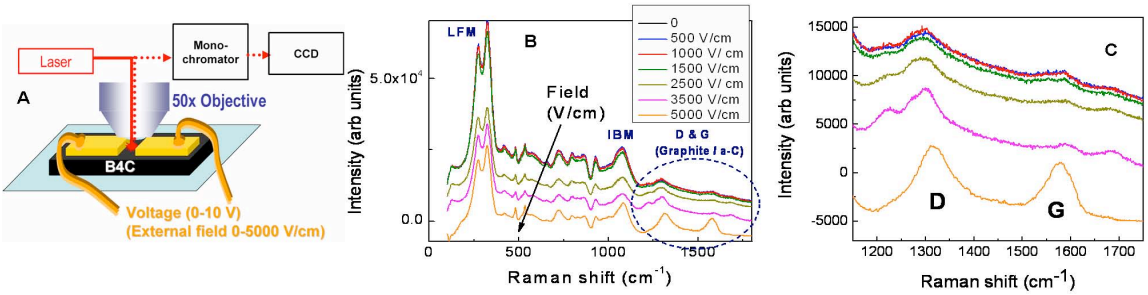

Figure 10: (a) Schematic of the electrical Raman experiment where a voltage pulse is applied while monitoring the change in the amorphous carbon content. (b) Raman spectra as a function of the applied electric field. (c) Raman spectra showing the increase in D and G peaks of carbon with electric field.

The Raman spectra of hot pressed B_4C, recorded *in-situ* during application of increasing electric field pulses are shown in Figure 10b and 10c. Two primary effects on the Raman spectra with increasing electric fields are evident. First, the decrease in the intensity of the B_4C related Raman modes (frequencies ranging from 275 cm^{-1} to 1100 cm^{-1}) can be seen; Second, the strong increase of the D (~1300 cm^{-1}) and G (~1600 cm^{-1}) carbon modes under voltage pulses can be observed in Figure 10c. It is also clear in Figure 10c that weak carbon D and G modes are present in the sample even before electric field is applied. In Figure 10c, both the Raman D and G modes strongly increase in intensity with electric field strength, especially between 1500 and 3500 V/cm, where the intensity of the B_4C modes (Figure 10b) was observed to decrease. Furthermore, the broad line widths of the peaks indicate the presence of amorphized carbon domains, rather than ordered graphite. Closer analysis of the data in Figure 10c reveals that the D peak increases faster in area and intensity than the G-peak, leading to an increase in the D/G ratio. Since the D/G intensities ratio in amorphous carbon is proportional to the size L of the graphitic domains through the relationship $ID/IG \sim L^2$, it can be inferred that the island sizes increase with electric field.

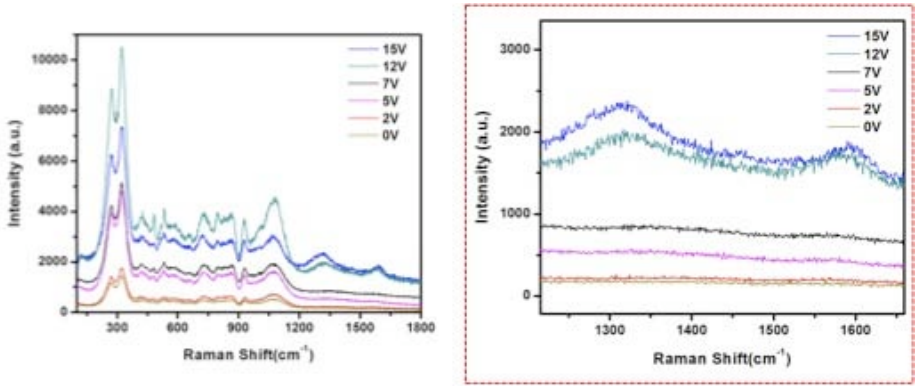

Figure 11: Electrical Raman measurements on SPS consolidated Si-doped B4C as a function of the applied electric field. The gap between the electrodes was 10 microns. The onset of amorphization was found to occur at 7V.

The electrical Raman measurements on the SPS consolidated Si-doped B_4C are shown in Figure 11. Two striking differences in the Raman spectra of these samples in comparison to hot pressed non Si doped B_4C can be observed. The first is the absence of amorphous carbon in the as consolidated samples (the 0V sample in Figure 11). As shown in Figure 9, amorphous carbon is almost always present in commercially available boron carbide powders and hot pressed samples. Second, the onset of amorphization in Si-doped B_4C consolidated with SPS does not occur until an electrical field of 7000 V/cm, which is higher by a factor of four compared to the hot pressed sample in Figure 10. Thus, at least for these measurements, the SPS of Si-doped B_4C appears to substantially improve the structural integrity of the boron carbide lattice, consistent with our theoretical calculations.

Additional insight into the ability for Si-doped B4C to withstand loading was obtained by performing indentation tests (100 – 300g Loads). Postmortem Raman on the indents provided additional information. The aim of the indents was not to obtain hardness values but to monitor structural transformation, and in particular amorphization. The Raman spectra from the damaged indented region are shown in Figure 12, for a SPS consolidated Si-doped B_4C and a commercial hot pressed B_4C sample. It can be clearly observed that under similar indentation and Raman measurement conditions, amorphization as indicated by the intensities of the carbon D and G peaks is dramatically suppressed in the Si-doped sample (red curve).

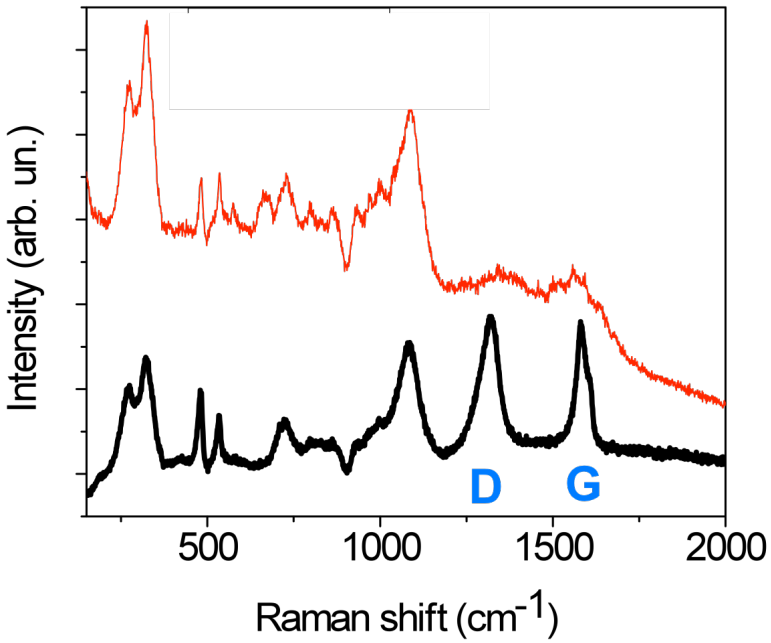

Figure 12: Raman spectra from the damaged indented regions for SPS consolidated Si-doped B_4C (red curve) and commercially available hot pressed sample (black curve).

Future Work

The preliminary study has yielded remarkably optimistic results for suppression of amorphization during electrical and mechanical loading by utilizing Si-doped B_4C nanostructures as the starting powder and subsequent consolidation by SPS. It has been widely believed that failure in B_4C occurs via shock induced amorphization and therefore absence of this feature in Si-doped B_4C is certainly a reason for hope. There are several challenges that must be confronted in moving forward. The first will be to repduciby fabricate sizable amount of silicon doped boron carbide powder and then utilize novel fabrication methods (such as free casting along with spark plasma sintering) to achieve materials that are dynamically shock resistant and also potentially tough. At present, the synthesis method is limited to academic quantities and must be scaled up if large quantities are to be realized. The second challenge is to determine the dynamic properties of the Si-doped B_4C samples. This could be done through modification of the electrical Raman measurements. We envision that it is possible to apply voltage pulses ranging from pico- to nano-seconds and monitor the structural evolution of the boron carbide. This will provide insight into the fast structural transformations that may occur in ballistic tests. It may also be possible to correlate the electric field strength to mechanical force applied to the material through ongoing theoretical simulations.

References:

1. G Fanchini, J W McCauley, and M Chhowalla, Phys. Rev. Lett. 97, 035502 (2006)
2. M. Chen, J. McCauley, and K. Hemker, Science 299, 1563 (2003).

3. D. Ghosh, G. Subhash, C. H. Lee, and Y. K. Yap, Appl. Phys. Lett., 91, 61910 (2007).
4. D Ge, V Dominich, T Juliano, E A Stach and Y Gogotsi, Acta Mat. 52, 3921 (2004).